

To appear in The Astrophysical Journal (Letters)

IRAS 16293-2442B: A Compact, Possibly Isolated Protoplanetary Disk in a Class 0 Object

Luis F. Rodríguez, Laurent Loinard, and Paola D'Alessio

Centro de Radioastronomía y Astrofísica, UNAM, Apdo. Postal 3-72, Morelia, Michoacán, 58089 México

`l.rodriguez, l.loinard, p.dalessio@astrosmo.unam.mx`

and

David J. Wilner and Paul T. P. Ho

Harvard-Smithsonian Center for Astrophysics, 60 Garden Street, Cambridge, MA 02138, USA

`dwilner, ho@cfa.harvard.edu`

ABSTRACT

Theoretical arguments suggest that protoplanetary disks around young stars should start small and grow with the addition of high angular momentum material to reach the radii of several hundred AU that characterize the disks around optically visible T Tauri stars. Examples of much more compact disks, with radii much less than 100 AU, have been found around some very young stars, but in all cases tidal truncation from a near binary companion provides a ready explanation for the small disk size. We report here an example of a compact, possibly isolated disk around the class 0 object IRAS16293-2422B, which is thought to be among the youngest protostars known. This disk has a Gaussian half power radius of only ~ 8 AU, and a detailed, self-consistent, accretion disk model indicates an outer radius of only 26 AU. This discovery supports the notion that protoplanetary disks start small and grow with time, although other explanations for the compact size cannot be ruled out, including gravitational instability in its outer parts and tidal truncation from the close approach of a now distant stellar companion.

Subject headings: ISM: individual (IRAS 16293-2422) — stars: planetary systems: protoplanetary disks — stars: pre-main sequence

1. Introduction

During the last decade there has been an accumulation of images at radio, infrared, and optical wavelengths (e. g. Wilner et al. 2000; Padgett et al. 1999; Burrows et al. 1996) that substantiate the old expectation that young stars form surrounded by circumstellar disks of gas and dust from which planets may condense in the future. There has also been significant advance in determining the duration of the disk phase, with estimates in the range of 2 to 10 million years (Haisch, Lada, & Lada 2001; Armitage, Clarke, & Palla 2003), as well as in studying examples of old disks (e. g. Calvet et al. 2002; Aigen, Lunine, & Bendo 2003). However, little is known about the early stages of disk formation, largely because the disks develop deep within protostellar envelopes that are opaque except at long wavelengths. Fortunately, the development of the 7 mm system at the Very Large Array now enables high angular resolution observations that can penetrate through the envelopes of Class 0 sources into the inner region where disks form.

Until now, most of the disks with measured dimensions are associated with Class I or Class II sources and have radii of order 100 AU or larger (e. g. Padgett et al. 1999; Kitamura et al. 2002). There are theoretical clues that suggest that the Class 0 sources, the youngest protostars known, could possess smaller disks. However, since these are short-lived and relatively rare objects, solid observational evidence is difficult to find and still missing.

The centrifugal radius, the radius at which centrifugal support becomes important in infalling gas, sets a characteristic disk size. One expects that the size of a disk should be initially small and increase with time, as gas with progressively higher angular momentum falls into the disk (Terebey, Shu, & Cassen 1984; Ruden & Lin 1986; Lin & Pringle 1990).

Obviously, direct imaging of young stars in various evolutionary stages would be the best way to investigate if disks grow in size during the early stages of star formation. A handful of compact (i. e. with radii much smaller than 100 AU) disks have been imaged toward the young stars L1551 IRS5 (Rodríguez et al. 1998; radii of ~ 10 AU), L1527 (Loinard et al. 2002; radius of ~ 20 AU), and SVS 13 (Anglada et al. 2004; radius of ≤ 30 AU). However, in these cases a nearby companion has always been found that could be making the disks small by tidal truncation.

In this paper we report 7 mm observations of IRAS 16293-2422B, a class 0 object located in the Ophiuchus molecular complex at a distance of 120 pc (Knude & Hog 1998). Class 0 objects are extremely young stars, with an estimated age of less than $\simeq 10^4$ yr (André, Ward-Thompson, & Barsony 1993). Our observations reveal the first case of an isolated, compact protoplanetary disk around a class 0 star, a result that supports the hypothesis that disks start small and grow with evolution.

2. Observations

The 7 mm observations were carried out in 2003 June 22 using the Very Large Array (VLA) of the National Radio Astronomy Observatory (NRAO)¹. The array was then in the A configuration and we had excellent phase stability during the run. The longest baselines of the array reached ~ 36 km, while the shortest ones were ~ 0.7 km. These observations have an angular resolution of $\sim 0''.07$, unmatched at present in the millimeter regime, and provide detailed imaging of circumstellar structures.

For all observations we used the fast-switching technique that consists of rapidly alternating observations of the source and the phase calibrator with cycle time of 2 minutes. An effective bandwidth of 100 MHz with two circular polarizations was employed. The absolute amplitude calibrator was 1328+307 (adopted flux density of 1.45 Jy), used in conjunction with a source model provided by NRAO. The phase calibrator was 1622–253, with a bootstrapped flux density of 1.79 ± 0.02 Jy. The data were edited and calibrated using the software package Astronomical Image Processing System (AIPS) of NRAO. Cleaned maps were obtained using the task IMAGR of AIPS and natural weighting. An extended source was detected in association with the source IRAS 16293-2422B (see Figure 1).

3. Discussion

3.1. Dust Spectrum

The structure detected in association with IRAS 16293-2422B has a total flux density of 31 ± 1 mJy, as determined from the cumulative flux in annuli centered on the source. The error given for the total flux density is a formal error; the total error is dominated by systematics at a $\sim 5\%$ level.

To construct the spectral energy distribution of IRAS16293B, we combined our new 7 mm observation with data taken from the literature. For the 2.7 mm (107.75 GHz) point, we used the value obtained by Looney, Mundy & Welch (2000) when they restore their data to be most sensitive to compact structures, since this is the situation most similar to ours. It should be pointed out, however, that the 2.7 mm flux density does not change much when all angular scales are taken into account (it merely increases from 0.42 to 0.55 Jy). This suggests that as much as 75% of the millimeter emission in IRAS16293B does emanate from

¹NRAO is a facility of the National Science Foundation operated under cooperative agreement by Associated Universities, Inc.

the compact disk seen here at 7 mm. The 0.8 mm (354 GHz) data point was obtained by Kuan et al. (2004) with an angular resolution of $\sim 2''$. The centimeter flux densities were obtained from Wootten (1989), Loinard (2002), Estalella et al. (1991), and Mundy et al. (1992).

The spectrum shown in Figure 2 can be fitted with a single power law, $S_\nu \propto \nu^{2.6}$, for frequencies in the range of 8.45 to 107.75 GHz, indicating that dust emission is dominant even at the relatively low frequency of 8.45 GHz. It is only below 8.45 GHz that a significant free-free excess is evident. Estalella et al. (1991) had reached similar conclusions. We then conclude that the 7 mm data point falls in the wavelength regime dominated by dust.

3.2. Disk Structure

A Gaussian least-squares fit to the source gives a deconvolved HPFW of $\sim 0''.14$, with no clear indications of significant ellipticity. At a distance of 120 pc, this corresponds to a characteristic half power radius of about 8 AU. This value is much smaller than the radii of several hundred AU that have been reported in other more evolved sources (e. g. Yokogawa et al. 2001; Jayawardhana et al. 2002; Wolf, Padgett, & Stapelfeldt 2003). The deconvolved HPFW of the 7 mm emission of two disk sources at comparable distances, HL Tau and TW Hya, obtained with the same techniques described here (Wilner, Ho, & Rodríguez 1996; Wilner et al. 2000), correspond to characteristic radii of ~ 50 AU, significantly larger than the value of ~ 8 AU determined for IRAS 16203-2422B. The Gaussian least-squares fit accounts well for the emission within $\leq 0''.2$ from the center of the disk. However, there is faint, extended emission associated with the source. Of the total flux density of 31 ± 1 mJy, the Gaussian fit accounts only for 25 ± 1 mJy, suggesting that ~ 6 mJy, about 20% of the total flux density, comes from a structure at radii larger than $0''.2$. If this extended emission had circular symmetry, as the compact, central part of the source, we would have to reconsider the extent of the disk. However, our analysis clearly indicates that the extended emission is not circularly symmetric and must have a different origin than the disk. The lack of symmetry in the extended component is marginally evident in Figure 1, where we see faint emission beyond $0''.2$ from the center of the disk, to the NE and SW. A more conclusive way of studying the morphology of this faint extended emission is by determining the average flux density beam^{-1} in “slices” taken at different position angles in a ring going from $0''.2$ to $0''.6$. The inner ring radius was selected because the compact, bright disk seems to become undetectable at this radius in the 7 mm image (see Figure 1), and the outer ring radius was selected because the faint, extended structure seems to stop contributing significantly to the integrated flux density (see discussion and Figure 4 below). In Figure 3 we show

these average flux densities as a function of position angle, where it is evident that there is significant emission at position angles of $\sim 70^\circ \pm 45^\circ$ and $\sim 250^\circ \pm 45^\circ$, and little or no emission outside of these position angle ranges. At present the nature of this extended emission is unclear. It could be related to the complex outflow phenomena associated with this source, although the bipolar outflow associated with IRAS 16293-2422B is at a position angle of $\sim 110^\circ$ (Hirano et al. 2001).

3.3. Isolated Nature of the Source

We then conclude that the IRAS 16203-2422B disk is much smaller than the cases previously mentioned and more comparable in size with the tidally truncated disks found in young close binary systems (L1551 IRS5: Rodríguez et al. 1998; L1527: Loinard et al. 2002; SVS 13: Anglada et al. 2004). However, in IRAS 16203-2422B the nearest stellar object known is IRAS 16293-2422A (possibly a close binary system on its own, see Loinard 2002), that at a projected distance of 600 AU, appears incapable at present of explaining the small size of the disk in IRAS 16293-2422B by tidal truncation. For tidal truncation to be effective, the separation between the stars should be only a few times the radius of the disk (Artymowicz & Lubow 1994). However, IRAS 16203-2422A and IRAS 16203-2422B may form a system of high eccentricity that comes very close at periastron. The eccentricity of an elliptical orbit is $e = (d_a - d_p)/(d_a + d_p)$, where d_a is the separation between stars at apastron and d_p is the separation between stars at periastron. Assuming that the present observed projected separation between components A and B, $d_{obs} \simeq 600$ AU, is a lower limit for d_a and that the required separation for tidal truncation to be effective, $d_{tidal} \simeq 100$ AU, is of order of d_p , we find that the required eccentricity must be in the range $0.7 \leq e < 1.0$, making this explanation somewhat unlikely. It is interesting to point out that the image of IRAS 16203-2422B shown in Figure 1 has marginal evidence of a spiral-like structure, a phenomenon that can result from tidal interaction (Grady et al. 2001; Clampin et al. 2003; Artymowicz & Lubow 1994). On the other hand, IRAS 16293-2422B is firmly established as a class 0 object (André, Ward-Thompson, & Barsony 1993) with an age of less than 10^4 years and we tentatively attribute the compactness of its disk to the youth of the source.

4. Disk model

The Gaussian half power size is an underestimate of the outer radius of the disk because of the central rise of disk surface density and temperature (Mundy et al. 1996), and with the purpose of estimating more accurately the basic parameters of the disk, our observations

are compared to the model of a steady irradiated α -disk, of the kind usually used to describe disks around Classical T Tauri Stars and Herbig Ae/Be stars. The details of how the model is calculated are given elsewhere (D’Alessio et al. 1998, 1999, 2001, 2004). In summary, the disk is assumed to have a constant mass accretion rate, \dot{M} , and a viscosity coefficient given by $\nu_{turb} = \alpha c_s H$, where α is a free parameter, taken to be constant through the disk, c_s is the local sound speed and H is the local gas scale height. The disk is in Keplerian rotation and its self-gravity is neglected compared to the stellar gravity. In an α -disk, the \dot{M} and the parameter α are related to the disk mass surface density through the conservation of angular momentum flux, given by

$$\Sigma \approx \frac{\dot{M}\Omega_k}{3\pi\alpha c_s^2} \left[1 - \left(\frac{R_*}{R} \right)^{1/2} \right]. \quad (1)$$

We assume the central star has a mass $M_* = 0.8 M_\odot$ (Ceccarelli et al. 2000), and we adopt for it an effective temperature $T_* \sim 4000$ K, a stellar luminosity $L_* \sim 10 L_\odot$ and a radius $R_* \sim 6.7 R_\odot$, roughly consistent with pre-main sequence tracks in the HR diagram (Siess, Dufour & Forestini 2000). Adopting a system bolometric luminosity of $L_{bol} \sim 16 L_\odot$, the accretion luminosity is $L_{acc} = GM_*\dot{M}/R_* \sim 6 L_\odot$, implying a mass accretion rate $\dot{M} \sim 1.7 \times 10^{-6} M_\odot \text{year}^{-1}$. All these values are very uncertain, thus, the disk model we present here has only an illustrative purpose, mainly to show that the disk interpretation is consistent with the data.

The disk is being heated by local viscous dissipation and by external irradiation. Since the stellar and accretion luminosities are comparable, we assume that the disk is being irradiated by both, the central star and the accretion shocks at the stellar surface, where most of the accretion luminosity is released. For simplicity, the shocks are assumed to emit as a blackbody with $T_{shock} \sim 8000$ K (Calvet & Gullbring 1998; Gullbring et al. 2000) and to cover a few percent of the stellar surface to account for the assumed accretion luminosity.

The main opacity source of the disk is dust, and the disk structure and emergent intensity depends on the grain’s composition and size distribution. We assume that the disk has interstellar-like dust grains in its upper layers and a population of millimeter-sized grains in its midplane. The small grains at the disk atmosphere absorb efficiently radiation from the star and the accretion shocks, characterized by shorter wavelengths than the disk’s own radiation. On the other hand, the millimeter-sized grains at the midplane have a larger emissivity at $\lambda \sim \text{mm}$ than interstellar medium grains. This model with small and big dust grains has a larger emergent intensity at 7 mm than a model with only millimeter-sized grains everywhere, since such big grains are less effective for absorbing stellar radiation and heating the disk (D’Alessio et al. 2004). The steady disk models that fit better the

observations shown in Figure 4 have a maximum radius $R_d = 26$ AU and a mass in the range $M_d = 0.3 - 0.4 M_\odot$.

For larger distances, the contribution of the extended component described in §3 becomes important, accounting for ~ 6 mJy at $0''.6 = 72$ AU. Figure 4 shows that this extended component has a cumulative flux density that does not grow as fast with distance as what an extrapolation of the steady disk model predicts (roughly $F \propto R$). One possibility is that this extended component is the outer disk where the mass surface density decreases exponentially with radius, according to evolutive models that take into account the disk expansion to conserve the total angular momentum (Hartmann et al. 1998). Another possibility is that our steady model breaks down in the outer regions, because the disk self-gravity becomes important. One way to evaluate this is by calculating the Toomre parameter corresponding to the disk model which fits the observations, $Q = c_s \Omega_k / 2\pi G \Sigma$, where we take the sound speed c_s evaluated at the disk midplane. For $R \sim 26$ AU, $Q \sim 0.4 - 0.3$, implying that the outer disk is gravitationally unstable. This instability might be the origin of the non-axisymmetric structures we find in the extended region (e.g. Gammie 2001, Rice et al. 2003). Models in which self-gravity is not neglected and where the outer exponential- Σ region is included, should be used to further explore these possibilities.

5. Conclusions

In conclusion, the disk imaged around IRAS 16293-2422B appears to be much smaller than the disks detected in more evolved young stars. The lack of a nearby detectable companion suggests that this compactness is a result of the youth of the object and not of tidal truncation. However, we cannot rule out other possible mechanisms that may explain the compactness of this disk. For instance, the outer parts of the disk may be gravitationally unstable and may have collapsed to clumpy structures more difficult to detect. Also, the source IRAS 16293-2422A appears now to be too far from IRAS 16293-2422B to produce tidal truncation but it may approach significantly during periastron. More extensive, high angular resolution imaging of disks around young stars in various evolutionary stages are needed to critically test the possibilities hinted by our observations.

LL, LFR, and PD are grateful to CONACyT, México and DGAPA, UNAM for their support.

REFERENCES

- Aigen, L., Lunine, J. I., & Bendo, G. J. 2003, *ApJ*, 598, L51
- André, P., Ward-Thompson, D., & Barsony, M. 1993, *ApJ*, 406, 122
- Anglada, G., Rodríguez, L. F., Osorio, M., Torrelles, J. M., Estalella, R., Beltrán, M. T., & Ho, P. T. P. 2004, *ApJ*, 605, L137
- Armitage, P. J., Clarke, C. J., & Palla, F. 2003, *MNRAS*, 342, 1139
- Artymowicz, P. & Lubow, S. H. 1994, *ApJ*, 421, 651
- Beckwith, S. V. W., Sargent, A. I., Chini, R. S., & Güsten, R. 1990. *AJ*, 99, 924
- Burrows, C. J. et al. 1996, *ApJ*, 473, 437
- Calvet, N. & Gullbring, E. 1998, *ApJ*, 509, 802
- Calvet, N., D'Alessio, P., Hartmann, L., Wilner, D., Walsh, W., & Sitko, M. 2002, *ApJ*, 568, 1008
- Ceccarelli, C., Castets, A., Caux, E., Hollenbach, D., Loinard, L., Molinari, S., & Tielens, A. G. G. M. 2000, *A&A*, 355, 1129
- Clampin, M. et al. 2003, *AJ*, 126, 385
- D'Alessio, P., Canto, J., Calvet, N., & Lizano, S. 1998, *ApJ*, 500, 411
- D'Alessio, P., Calvet, N., Hartmann, L., Lizano, S., & Cantó, J. 1999, *ApJ*, 527, 893
- D'Alessio, P., Calvet, N., & Hartmann, L. 2001, *ApJ*, 553, 321
- D'Alessio, P., Calvet, N., Hartmann, L., Franco-Hernández, R., Sitko, M. & Servin, H. 2004, in preparation
- Estalella, R., Anglada, G., Rodríguez, L. F., & Garay, G. 1991, *ApJ*, 371, 626
- Gammie, C. F. 2001, *ApJ*, 553, 174
- Grady, C. A. et al. 2001, *AJ*, 122, 3396
- Gullbring, E., Calvet, N., Muzerolle, J., & Hartmann, L. 2000, *ApJ*, 544, 927
- Haisch, K. E., Lada, E. A., & Lada, C. J. 2001, *ApJ*, 553, L153

- Hartmann, L., Calvet, N., Gullbring, E., & D'Alessio, P. 1998, *ApJ*, 495, 385
- Hirano, N., Mikami, H., Umemoto, T., Yamaoto, S., & Taniguchi, Y. 2001, *ApJ*, 547, 899
- Jayawardhana, R., Luhman, K. L., D'Alessio, P., & Stauffer, J. R. 2002, *ApJ*, 571, L51
- Kitamura, Y., Momose, M., Yokogawa, S., Kawabe, R., Tamura, M., & Ida, S. 2002, *ApJ*, 581, 357
- Knude, J. & Hog, E. 1998, *A&A*, 338, 897
- Kuan, Y.-J., Huang, H.-C., Charnley, S. B., Hirano, N., Takakuwa, S., Wilner, D. J., Liu, S.-Y., Ohashi, N., Bourke, T. L., Qi, C., & Zhang, Q. 2004, *ApJ*, 616, L27
- Lin, D. N. C. & Pringle, J. E. 1990, *ApJ*, 358, 515
- Loinard, L. 2002, *RevMexA&A*, 38, 61
- Loinard, L., Rodríguez, L. F., D'Alessio, P., Wilner, D. J., & Ho, P. T. P. 2002, *ApJ*, 581, L109
- Looney, L. W., Mundy, L. G., & Welch, W. J. 2000, *ApJ*, 529, 477
- Mundy, L. G., Walking, B. A., Blake, G. A., & Sargent, A. I. 1992, *ApJ*, 385, 306
- Mundy, L. G., Looney, L. W., Erickson, W., Grossman, A., Welch, W. J., Forster, J. R., Wright, M. C. H., Plambeck, R. L., Lugten, J., & Thornton, D. D. 1996, *ApJ*, 464, L169
- Padgett, D. L., Brandner, W., Stapelfeldt, K. R., Strom, S. E., Terebey, S., & Koerner, D. 1999, *AJ*, 117, 1490
- Rice, W. K. M., Armitage, P. J., Bate, M. R., & Bonnell, I. A. 2003, *MNRAS*, 339, 1025
- Rodríguez, L. F. et al. 1998, *Nature*, 395, 355
- Ruden, S. P. & Lin, D. N. C., 1986, *ApJ*, 308, 883
- Siess, L., Dufour, E., & Forestini, M. 2000, *A&A*, 358, 593
- Terebey, S., Shu, F. H., & Cassen, P. 1984, *ApJ*, 286, 529
- Wilner, D. J., Ho, P. T. P., & Rodríguez, L. F. 1996, *ApJ*, 470, L117
- Wilner, D. J., Ho, P. T. P., Kastner, J. H., & Rodríguez, L. F. 2000, *ApJ*, 534, L101

Wolf, S., Padgett, D. L., & Stapelfeldt, K. R. 2003, ApJ, 588, 373

Wootten, A. 1989, ApJ, 337, 858

Yokogawa, S., Kitamura, Y., Momose, M., Asaki, Y., Tamura, M., Ida, S., & Kawabe, R.
2001, ApJ, 552, L59

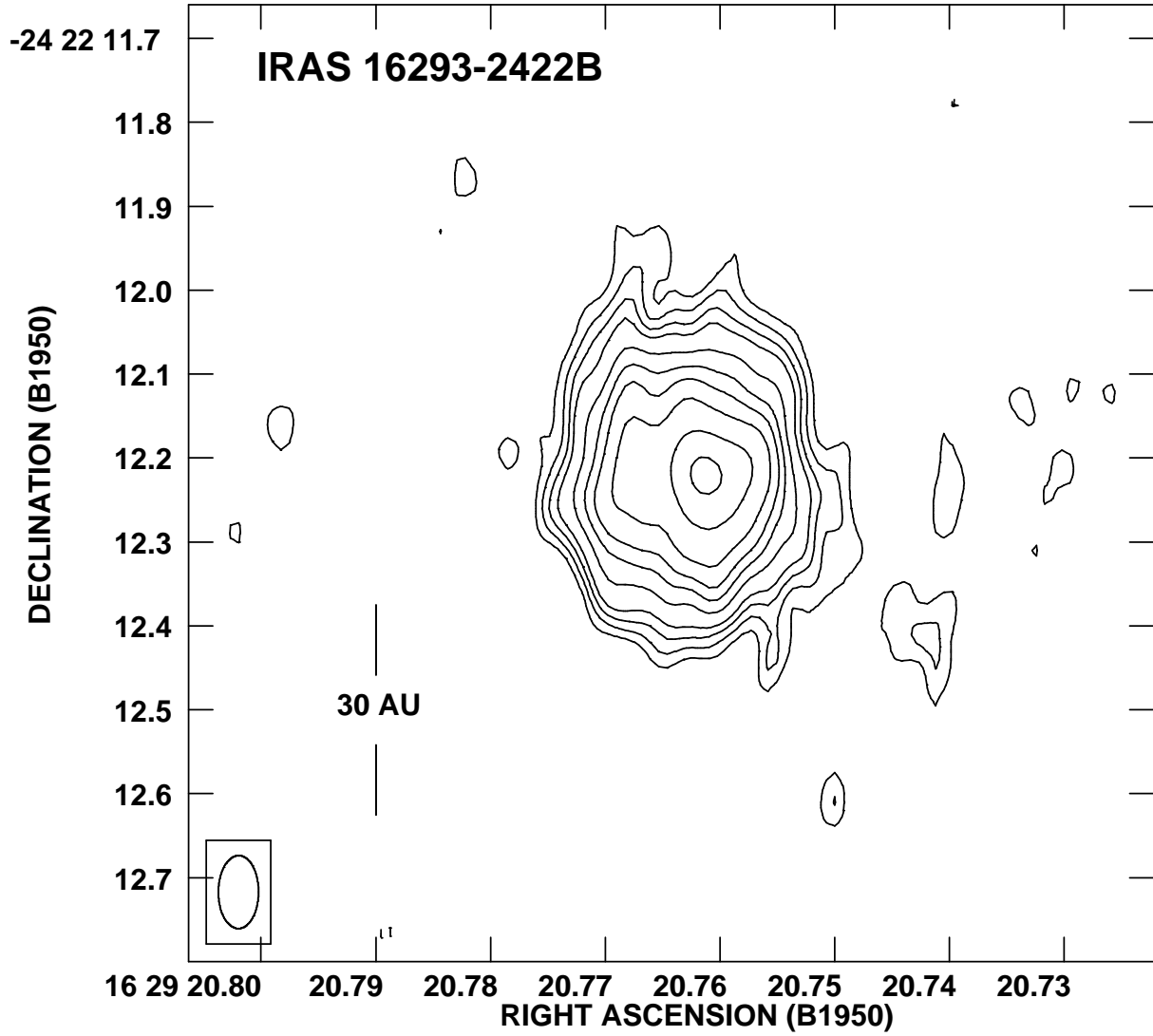


Fig. 1.— VLA image at 7 mm of IRAS 16293-2422B. Contours are -3, 3, 4, 5, 6, 8, 10, 12, 15, 20, and 25 times $0.1 \text{ mJy beam}^{-1}$, the rms of the image. The half power contour of the synthesized beam ($0''.09 \times 0''.05$; $\text{PA} = 0^\circ$) is shown in the bottom left corner.

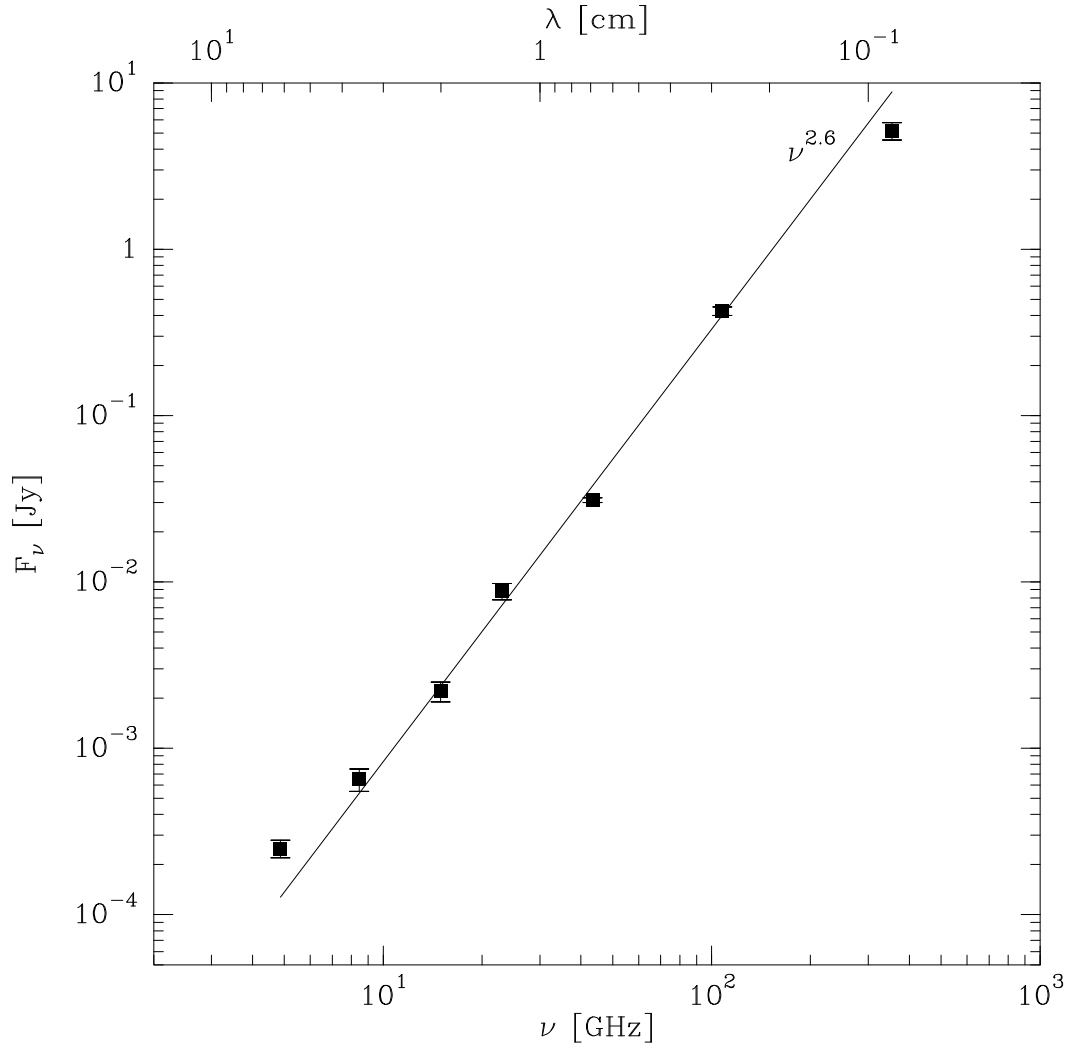


Fig. 2.— Centimeter and millimeter spectrum of IRAS 16293-2422B.

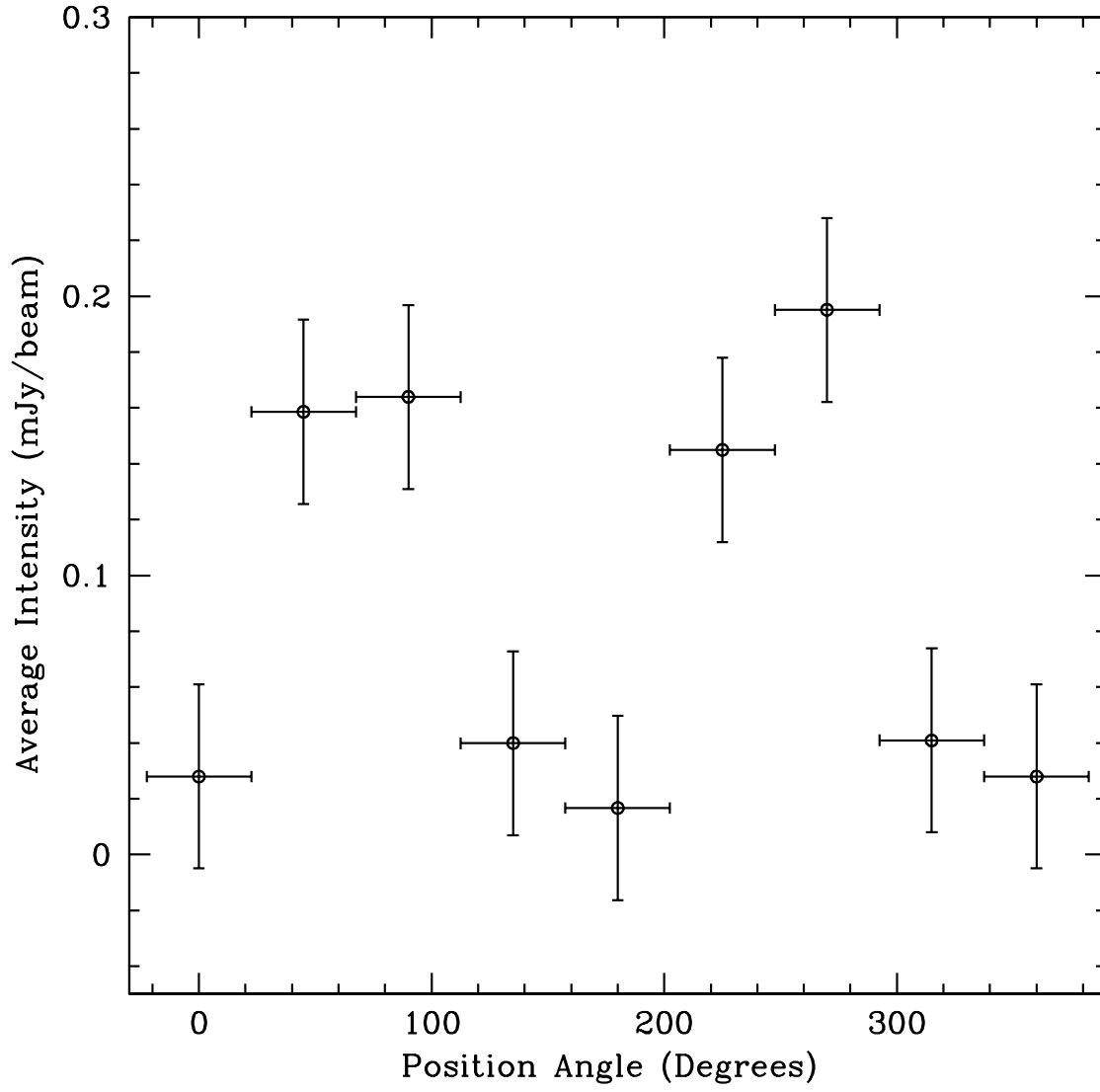


Fig. 3.— Average intensity (mJy beam^{-1}) as a function of position angle (degrees) in a ring with radius from $0''.2$ to $0''.6$ for the 7 mm source associated with IRAS 16293-2422B. Note the presence of emission at $\sim 70^\circ \pm 45^\circ$ and $\sim 250^\circ \pm 45^\circ$.

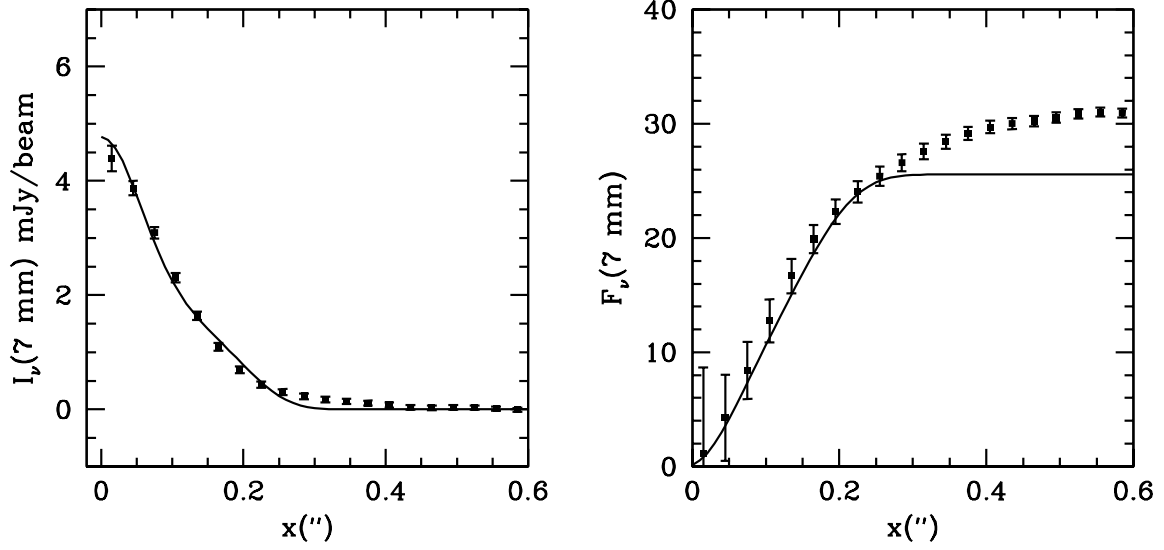


Fig. 4.— The left panel shows the radial profile of the azimuthally averaged emergent intensity at 7 mm, calculated adopting a $0''.1$ circular beam. The right panel shows the cumulative flux at 7 mm as a function of the radial distance to the center of the disk.